

AD-A115 818

NATIONAL BUREAU OF STANDARDS BOULDER CO QUANTUM PHYS--ETC F/6 20/7
ELECTRON EXCITATION OF O(2) METASTABLES IN O(2)-N(2) MIXTURES A--ETC(U)
MAY 82 C YAMABE, A V PHELPS MIPR-FY1455-81-00605

UNCLASSIFIED

AFWAL-TR-82-2016

NL

1 OF 1
AD-A
*68:8

END

DATE

FILED

87-82

DTIC

AD A115818

AFWAL-TR-82-2016



ELECTRON EXCITATION OF O_2 METASTABLES IN O_2-N_2 MIXTURES AND OF
FREE-FREE RADIATION IN ARGON

C. YAMABE AND A. V. PHELPS

QUANTUM PHYSICS DIVISION
U.S. BUREAU OF STANDARDS
BOULDER, CO 80303

May 1982

FINAL REPORT FOR PERIOD OCTOBER 1980 - SEPTEMBER 1981

Approved for public release; distribution unlimited

AERO PROPULSION LABORATORY
AIR FORCE WRIGHT AERONAUTICAL LABORATORIES
AIR FORCE SYSTEMS COMMAND
WRIGHT-PATTERSON AIR FORCE BASE, OHIO 45433

DTIC
ELECTE
JUN 21 1982
S D B

82 142

NOTICE


When Government drawings, specifications, or other data are used for any purpose other than in connection with a definitely related Government procurement operation, the United States Government thereby incurs no responsibility nor any obligation whatsoever; and the fact that the government may have formulated, furnished, or in any way supplied the said drawings, specifications, or other data, is not to be regarded by implication or otherwise as in any manner licensing the holder or any other person or corporation, or conveying any rights or permission to manufacture use, or sell any patented invention that may in any way be related thereto.

This report has been reviewed by the Office of Public Affairs (ASD/PA) and is releasable to the National Technical Information Service (NTIS). At NTIS, it will be available to the general public, including foreign nations.

This technical report has been reviewed and is approved for publication.



ALLAN GARSCADDEN
Project Engineer



DONALD P. MORTEL
Chief, Energy Conversion Branch
Aerospace Power Division
Aero Propulsion Laboratory

FOR THE COMMANDER



JAMES D. REAMS
Chief, Aerospace Power Division
Aero Propulsion Laboratory

"If your address has changed, if you wish to be removed from our mailing list, or if the addressee is no longer employed by your organization please notify POOC-3, W-PAFB, OH 45433 to help us maintain a current mailing list".

Copies of this report should not be returned unless return is required by security considerations, contractual obligations, or notice on a specific document.

Unclassified

SECURITY CLASSIFICATION OF THIS PAGE (When Data Entered)

REPORT DOCUMENTATION PAGE		READ INSTRUCTIONS BEFORE COMPLETING FORM
1. REPORT NUMBER AFWAL-TR-82-2016	2. GOVT ACCESSION NO. AD A115 818	3. RECIPIENT'S CATALOG NUMBER
4. TITLE (and Subtitle) ELECTRON EXCITATION OF O_2 METASTABLES IN O_2 - N_2 MIXTURES AND OF FREE-FREE RADIATION IN ARGON		5. TYPE OF REPORT & PERIOD COVERED Final Oct. 80-Sept. 81
		6. PERFORMING ORG. REPORT NUMBER
7. AUTHOR(s) C. Yamabe and A. V. Phelps		8. CONTRACT OR GRANT NUMBER(s) MIPR FY1455-81-00605
9. PERFORMING ORGANIZATION NAME AND ADDRESS Quantum Physics Division U.S. Bureau of Standards Boulder, CO 80303		10. PROGRAM ELEMENT, PROJECT, TASK AREA & WORK UNIT NUMBERS 2301S208
11. CONTROLLING OFFICE NAME AND ADDRESS Aero Propulsion Laboratory (AFWAL/POOC) Air Force Wright Aeronautical Laboratories (AFSC) Wright-Patterson AFB, OH 45433		12. REPORT DATE May 1982
		13. NUMBER OF PAGES 32
14. MONITORING AGENCY NAME & ADDRESS (if different from Controlling Office)		15. SECURITY CLASS. (of this report) Unclassified
		15a. DECLASSIFICATION/DOWNGRADING SCHEDULE
16. DISTRIBUTION STATEMENT (of this Report) Approved for public release; distribution unlimited.		
17. DISTRIBUTION STATEMENT (of the abstract entered in Block 20, if different from Report)		
18. SUPPLEMENTARY NOTES		
19. KEY WORDS (Continue on reverse side if necessary and identify by block number) oxygen, nitrogen, argon, metastable, electrons, radiation, quenching, excitation coefficient, free-free radiation		
20. ABSTRACT (Continue on reverse side if necessary and identify by block number) Measurements have been made of electron excitation coefficients for the production of $O_2(a^1\Delta)$ metastables in mixtures of O_2 and N_2 for a range of mixture ratios and mean electron energies. The results are in agreement with calculations using the best available electron collision cross sections sets provided proper allowance is made for cascading from high excited states. Measurements have been made of coefficients for the production of free-free photons (Bremsstrahlung) as a result of the collisions of electrons with argon atoms. These measurements were made under the carefully controlled (continued over)		

DD FORM 1 JAN 73 1473 EDITION OF 1 NOV 65 IS OBSOLETE

Unclassified

SECURITY CLASSIFICATION OF THIS PAGE (When Data Entered)

20. (continued):

conditions of the electron drift tube. The mean electron energy was varied from 1.4 to 4.2 eV and the wavelength was varied from 500 nm to 1.3 nm. The results are in agreement with theory to within the experimental uncertainty of $\pm 20\%$.

PREFACE

This work was performed in the Quantum Physics Division, U.S. Bureau of Standards, at the Joint Institute for Laboratory Astrophysics under MIPR FY1455-81-00605. Dr. Yamabe was at the Joint Institute for Laboratory Astrophysics while on leave from the Electrical Engineering Department, Nagoya University, Nagoya, Japan. This work was performed during the period October 1980 through September 1981 under Project 2301 Task S2, "Plasma Research, Gas Discharge and Laser Plasmas." The Air Force contract manager was Dr. Alan Garscadden, Energy Conversion Branch, Aero Propulsion Laboratory.

Accession For	
NTIS GRA&I	<input checked="" type="checkbox"/>
DTIC TAB	<input type="checkbox"/>
Unannounced	<input type="checkbox"/>
Justification	
By	
Distribution/	
Availability Codes	
Dist	Avail and/or Special
A	

111 /iv



TABLE OF CONTENTS

<u>Section</u>	<u>Page</u>
I. INTRODUCTION	1
II. THEORY OF MEASUREMENTS	3
III. EXPERIMENTAL APPARATUS AND PROCEDURE	12
IV. $O_2(a^1\Delta)$ EXCITATION COEFFICIENTS.	14
V. FREE-FREE EMISSION COEFFICIENTS.	21
VI. SUMMARY AND RECOMMENDATION	28
APPENDIX	30
REFERENCES	31

LIST OF ILLUSTRATIONS

<u>Figure</u>	<u>Page</u>
1. Schematic of experiment.	4
2. Rate coefficients per $O_2(a^1\Delta)$ metastables vs average electron energy in O_2 - N_2 -Ar mixtures. The symbols and the corresponding percentages of O_2 , N_2 and Ar are: ■, 1-1-98; ●, 1-2-97; ▼, 1-5-94; ▲, 2-10-88; o, 5-5-90.	15
3. Excitation coefficients for production of $O_2(a^1\Delta)$ metastables in pure O_2 and in 20% O_2 - 80% N_2	19
4. Infrared emission transient near 1.3 μm from 0.05% O_2 in Ar.	22
5. Free-free emission coefficient per fractional bandwidth for electrons in argon vs E/N	23
6. Wavelength dependence of free-free emission coefficient per fractional bandwidth for electrons in Ar.	25
7. Theoretical cross section per fractional bandwidth for the emission of 1.78 eV photons vs electron energy.	26

LIST OF TABLES

<u>Table</u>	<u>Page</u>
1. Rate Coefficients for Quenching of Excited Oxygen	17
2. Calculated Fractional Excitation Transfer Efficiencies	17

SECTION I

INTRODUCTION

This report describes measurements of two important kinds of electron collisions with gas atoms and molecules. One of these is collisions of electrons with oxygen molecules resulting in the production of the lowest metastable state of the oxygen molecule, i.e., the $a^1\Delta_g$ state. The second process is the production of free-free radiation in collisions of electrons with argon atoms, i.e. the collisions of electrons with atoms resulting in the production of photons with a wide range of wavelengths.

Electron collisions with the oxygen molecule are an important energy loss mechanism in the earth's ionosphere¹ and in the plasmas produced by charged particle beams.² In addition, some of the excited states produced by these collisions are potentially important sources of stored energy, e.g., the oxygen molecules in the lowest metastable state $a^1\Delta_g$ can efficiently transfer energy to iodine and so excite the atom.³ In this report we describe the extension of our earlier^{4,5} measurements of the excitation of $O_2(a^1\Delta)$ metastables in O_2 -Ar mixtures to include measurements in O_2 - N_2 -Ar and O_2 - N_2 mixtures.

The measurement of emission coefficients for the production of free-free radiation in collisions between electrons and argon atoms was an unexpected bonus for the present drift tube experiments. As will be discussed in Section IV, the collision cross sections and associated emission coefficients for this process are much smaller than molecular metastable excitation coefficients, e.g., the maximum value of the free-free excitation coefficient for our 1.3 μ m detection system is 10^{-3} to 10^{-4} of the maximum

value for excitation of the $O_2(a^1\Delta)$ metastable. This low ratio is roughly balanced out by the fact that every infrared or visible photon produced by the free-free process is emitted from the drift tube whereas a maximum of about 1 in 2000 of the $O_2(a^1\Delta)$ metastables escapes quenching and emits a photon. These measurements of free-free radiation are of special significance because for the first time one can make measurements under well controlled conditions of the absolute intensities of the free-free radiation produced by electron collisions with atoms and molecules. The resultant data is of importance because of the usefulness of free-free radiation as a diagnostic technique^{6,7} and because free-free radiation can be a significant source of emitted radiation in a low mean-energy, high electron density plasma.⁸ One property of free-free radiation which has only begun to be exploited is absence of a delay time between the electron-atom collision and the emission of a photon.

Section II of this report contains a discussion of the experimental technique and of the models used to interpret the observed signals. Section III contains a brief review of the experimental apparatus and of the data processing. The results of the measurements of the excitation coefficients for the $O_2(a^1\Delta)$ state in O_2-N_2 -Ar and O_2-N_2 mixtures are presented in Section IV. In Section V we summarize the measurements of the free-free emission coefficients for electrons in Ar and compare these results with theoretical predictions. Our conclusions and recommendations are presented in Section VI.

SECTION II

THEORY OF THE MEASUREMENTS

A schematic of the drift tube technique used for determination of excitation and emission coefficients is shown in Fig. 1. UV radiation from a continuously operating 100 W high pressure mercury lamp is passed through broad band interference filters centered at 190 nm and then through a quartz window coated on the inside with a semi-transparent, cathode film of evaporated Pd-Au. The resulting photoelectrons enter the gas-filled, parallel plate drift tube. The anode voltage is modulated so as to periodically apply a known electric field E and so produce electrons with a modulated mean energy. These electrons may excite the O_2 molecules to the $a^1\Delta_g$ state which can radiate photons at 1.27 μm in forbidden transitions to the $X^3\Sigma_g^-$ ground state of O_2 . Since the radiative lifetime of these metastables is very long⁹ (3900 sec), most of the metastables will be destroyed by diffusion to the drift tube electrodes or by collisional quenching. A high density of Ar atoms is used to reduce the diffusion loss. At best, about one molecule in 2000 is able to radiate at 1.27 μm . In about one out of 10^8 collisions between electrons and argon atoms a free-free photon is emitted and leaves the drift tube. When the ratio of the argon density to the oxygen density is large, e.g., 2000:1, the free-free emission is comparable with the 1.27 μm emission.

1. Oxygen measurements

Since the theory of this experiment has been discussed in detail in the previous final report⁴ and has been published⁵, we will give only a very brief review in this report. The radiated power P at 1.27 μm reaching the

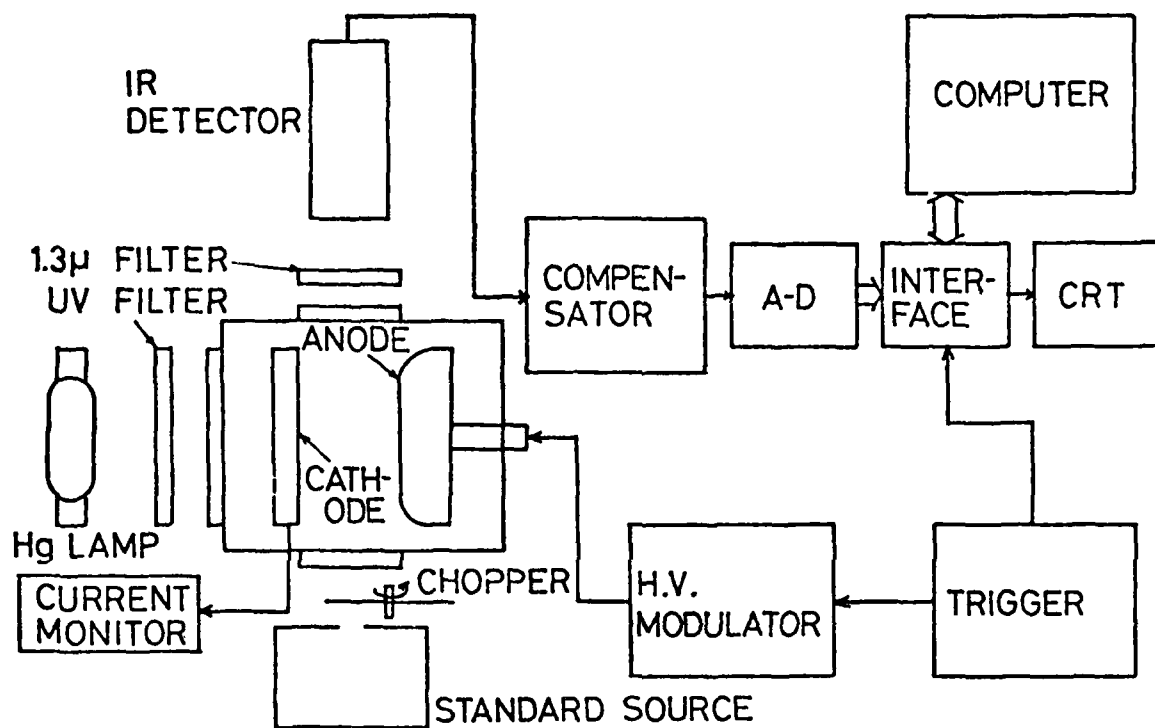


Figure 1. Schematic of experiment.

detector from the drift tube in the absence of filters, etc. is given by

$$P = h\nu A \frac{\Delta\Omega}{4\pi} \int_V \eta[a] dV, \quad (1)$$

where $h\nu$ is the photon energy, A is the measured radiative transition probability as corrected for collision induced radiation by the buffer gas,^{9,10} $\Delta\Omega$ is the solid angle of the detector as seen from the center of the drift tube and η is the efficiency of photon collection from various parts of the drift tube relative to that at the center. The density of $O_2(a^1\Delta_g)$ metastables $[a]$ is obtained from the solution of the continuity equation

$$\frac{\partial [a]}{\partial t} = D\nabla^2[a] - (k_d N + A)[a] + k_e n_e, \quad (2)$$

where D is the effective metastable diffusion coefficient for the mixture, k_d is the effective rate coefficient for metastable destruction by O_2 and by Ar at the total gas density N , and n_e is the electron density. Here the electron excitation rate coefficient k_e is given by

$$k_e = \int_0^\infty v Q_a(\epsilon) \epsilon^{1/2} f(\epsilon) d\epsilon, \quad (3)$$

where v and ϵ are the electron speed and energy, $Q_a(\epsilon)$ is the cross section for electron excitation of the $O_2(a^1\Delta_g)$ state, and $f(\epsilon)$ is the normalized electron energy distribution appropriate to the O_2 -Ar mixture and to the value of E/N used. Here we assume that any excitation of the $O_2(a^1\Delta_g)$ state by cascading from higher excited states is rapid on the time scale of these experiments and is included in k_e .

The coefficients describing the destruction of metastables in this experiment are determined from measurements of the time dependence of the 1.27 μm emission. The diffusion term in Eq. (2) adds greatly to the difficulty

of quantitative analysis of the emission data and the reader is referred to reference 11 for a detailed discussion. For the present purposes we will limit the discussion to high gas densities where

$$k_d N \gg A + D(\pi/L)^2, \quad (4)$$

where L is the distance between the drift tube electrodes. In this limit the metastable density is given by

$$[a] = \frac{k_e N n_e}{\gamma} (1 - e^{-\gamma t}) = \frac{\alpha i}{e \gamma A_c} (1 - e^{-\gamma t}), \quad (5)$$

where $k_e N = \alpha w_e$, e and w_e are the electron charge and drift velocity, i is the total current, $\gamma = k_d N$ is the decay constant and A_c is the area of the cathode. The radiated power is a maximum P_{\max} when $[a] = \alpha i / e \gamma A_c$.

Equations (1) and (5) yield an expression for α/N in terms of the directly measured quantities P_{\max} , γ , i , and L and the calculated current correction factor q and geometrical correction factor G . Thus, at high gas densities α/N is given by

$$\frac{\alpha}{N} = \frac{e \gamma q}{A L N G i} \frac{4 \pi}{\Delta \Omega} \frac{P_{\max}}{h \nu}. \quad (6)$$

The reader is referred to reference 11 for the general formula for α/N and for a discussion of the effects of diffusion, the definitions of q and G , etc.

The (0-0) band of the $a^1\Delta_g - X^3\Sigma_g^+$ system at $1.27 \mu\text{m}$ was isolated from most of the scattered radiation from the UV lamp by an interference filter with 75% peak transmission at $1.32 \mu\text{m}$ and a $0.147 \mu\text{m}$ FWHM. The value $\langle f_1 \rangle$ of the filter transmission function was calculated⁷ using the emission band profile of Wood, et al.¹² and the measured filter transmission. As discussed previously^{4,5} the near coincidence of wavelengths and transition probabilities for the 0-0 and 1-1 transitions means that our measurements are independent

of the ratio of populations in the $v=1$ and $v=0$ levels of the $O_2(a^1\Delta)$ state. Self absorption of the $1.27 \mu m$ radiation by the O_2 is negligible for the low O_2 densities of these experiments.⁹

2. Free-free emission measurement

For our purposes it is convenient to divide the free-free emission continuum into a number of spectral bands of frequency width $d\nu$ and to regard the collision process leading to emission of radiation in this band as an inelastic collision process for the electrons in the drift tube. The spectral intensity I_ν in units of photons per unit volume and per unit frequency interval per sec is given by^{6,7}

$$I_\nu d\nu = n_e N \frac{d\nu}{\nu} \int_0^\infty \nu Q_{ff}(\epsilon) \epsilon^{1/2} f(\epsilon) d\epsilon \equiv k_{ff}(\nu) n_e N \frac{d\nu}{\nu}. \quad (7)$$

Here again n_e and N are the electron and neutral atom or molecule densities, $f(\epsilon)$ is the normalized electron energy distribution and $Q_{ff}(\epsilon, h\nu)$ is the cross section for emission of a photon of energy $h\nu$ by the free-free process. The results of various theoretical calculations of $Q_{ff}(\epsilon)$ for electrons in argon are discussed in Section IV.

The signal reaching the photon detector is obtained by integrating Eq. (1) over the drift tube volume and over frequency, i.e.,

$$S_{ff} = \iint \frac{d\nu}{\nu} dV k_{ff}(\nu) n_e N f_w(\nu) D(\nu) f_i(\nu) \frac{\Delta\Omega_c}{4\pi} \eta, \quad (8)$$

where $f_w(\epsilon)$ is the fractional transmission of the windows between the collision chamber and the detector, $D(\nu)$ is the responsivity of the detector per photon, amplifier and recording system as a function of ν , $f_i(\nu)$ is the fractional transmission of the interference or other filter inserted between the collision chamber and the detector, $\Delta\Omega_c$ is the solid angle of the detector as seen from the center of the collision chamber, and η is the efficiency

of the detection system at various points in the collision chamber relative to that at the center of the chamber.¹¹

Equation (8) can be rewritten as

$$S_{ff} = \frac{N\Delta\Omega}{4\pi} \frac{c}{\int_0^\infty f_w(v) k_{ff}(v) D(v) f_i(v) \frac{dv}{v} \times \int_V n_e \eta dV} . \quad (9)$$

We define a geometrical factor G_{ff} by the relation

$$G_{ff} = \frac{\int_V n_e \eta dV}{\int_V n_e dV} . \quad (10)$$

We note that G_{ff} is equal to the G factor defined by Lawton and Phelps¹¹ in the limit of no diffusion, i.e., $D \rightarrow 0$. This factor is evaluated in the Appendix of this report. In the usual case of a slow variation in f_w , $k_{ff}(v)$ and $D(v)$ with v compared to that of $f_i(v)$, the integral over v can be written as $f_w(v_0)k_{ff}(v_0)D(v_0)\langle f_i \rangle \Delta v$. Here $\langle f_i \rangle \Delta v$ is the "area" under the filter transmission curve.

Since the electron density varies as $n_e = n_0 \exp(ax/L)$, Eq. (9) can now be written as

$$S_{ff} = \frac{N\Delta\Omega}{4\pi} \frac{G_{ff}}{a} \frac{(1-e^{-a})}{a} \frac{i_c L}{e w_e} f_w(v_0) k_{ff}(v_0) D(v_0) \langle f_i \rangle \frac{\Delta v}{v} , \quad (11)$$

where $a = (\alpha_a - \alpha_i)L$, α_a and α_i are the attachment and ionization coefficients per unit distance, L is the separation of the cathode and anode of the drift tube, i_c is the electron current leaving the cathode and e and w_e are the electron charge and drift velocity. As discussed previously,¹¹ we replace the electron component of the drift tube current $i_c(1-e^{-a})/a$ by i/q , where i is the total drift tube current and

$$q = (\alpha_a L - \alpha_i L e^{-a}) (1-e^{-a})^{-1} . \quad (12)$$

The quantity q is to be calculated from separate measurements or calculations of α_a and α_i .

Next we recall that the reference signal S_r reaching the detector from the black-body or incandescent source is given by

$$S_r = \Delta\Omega_r a_r \int_0^\infty f_r(\nu) f_e(\nu) \epsilon(\nu) B(\nu) D(\nu) f_i(\nu) d\nu, \quad (13)$$

where $\Delta\Omega_r$ is the solid angle of the detector as seen from a limiting aperture of area a_r , $f_r(\nu)$ is the transmission of the windows between the reference source and the collision chamber, $\epsilon(\nu)$ is the emissivity of the reference source, $B(\nu)d\nu$ number of photons per second emitted by a black-body per unit of surface and per unit solid angle. Here the reference source is assumed to be large enough to completely fill the aperture as seen from the detector. Using these relations we find that

$$\begin{aligned} \frac{S_{ff}}{S_r} &= \frac{N\Delta\Omega_c G_{ff}}{4\pi\Delta\Omega_r a_r} \frac{iL}{ew_e q} \frac{\int_0^\infty f_w(\nu) k_{ff}(\nu) D(\nu) f_i(\nu) d\nu/\nu}{\int_0^\infty f_r(\nu) f_w(\nu) \epsilon(\nu) B(\nu) D(\nu) f_i(\nu) d\nu} \\ &\approx \frac{N\Delta\Omega_c G_{ff}}{4\pi\Delta\Omega_r a_r} \frac{iL}{ew_e q} \frac{k_{ff}(\nu_i) \langle f_i \rangle (\Lambda\nu/\nu_i)}{f_r(\nu_i) \int \epsilon(\nu) B(\nu) f_i(\nu) d\nu}. \end{aligned} \quad (14)$$

If we define a free-free excitation coefficient $\alpha_{ff}(\nu_i)$ by

$$\alpha_{ff}(\nu_i) = k_{ff}(\nu_i) N/w_e, \quad (15)$$

then

$$\frac{\alpha_{ff}(\nu_i)}{N} = \frac{C_{ff} q S_{ff}}{G_{ff} i N S_r}, \quad (16)$$

where

$$C_{ff}(\nu_1) = \frac{4\pi\Delta\Omega_r e a_r}{\Delta\Omega_c L} \frac{\int_0^\infty f_r(\nu) f_w(\nu) \epsilon(\nu) B(\nu) D(\nu) f_1(\nu) d\nu}{\int_0^\infty f_w(\nu) \left[\frac{k_{ff}(\nu)}{k_{ff}(\nu_1)} \right] D(\nu) f_1(\nu) d\nu/\nu} \quad (17)$$

$$\approx \frac{4\pi\Delta\Omega_r e a_r f_r(\nu_1) \nu_1}{\Delta\Omega_c L \langle f_1 \rangle \Delta\nu} \int_0^\infty f_1(\nu) \epsilon(\nu) B(\nu) d\nu$$

or

$$C_{ff}(\lambda_1) = \frac{4\pi\Delta\Omega_r e a_r}{\Delta\Omega_c L} \frac{\int_0^\infty f_r(\lambda) f_w(\lambda) \epsilon(\lambda) B'(\lambda) D'(\lambda) f_1(\lambda) d\lambda}{\int_0^\infty f_w(\lambda) f_1(\lambda) \left[\frac{k_{ff}(c/\lambda)}{k_{ff}(c/\lambda_1)} \right] D'(\lambda) \frac{hc}{\lambda^2} d\lambda} \quad (18)$$

$$\approx \frac{4\pi\Delta\Omega_r a_r f_r(\lambda_1) \lambda_1}{\Delta\Omega_c L \langle f_1 \rangle / e} \frac{\int_0^\infty f_1(\lambda) \epsilon(\lambda) B'(\lambda) d\lambda}{\int_0^\infty f_1(\lambda) d\lambda}$$

where

$$D'(\lambda) = D(\lambda)/h\nu \quad \text{and} \quad h\nu B(\nu) d\nu = B'(\lambda) d\lambda.$$

We note that the formula for determining $\alpha_{ff}(\nu_1)/N$ from the experimental data, i.e. Eq. (16), is very much like Eq. (17) of Lawton and Phelps¹¹ for determining α_b/N for the $O_2(b^1\Sigma)$ metastables. Instead of the ratio of the metastable decay constant λ_1 to the radiative transition probability A , Eq. (14) contains the ratio $\Delta\nu/\nu_1$. The constant C given by Eqs. (17) and (18) is the same as for Lawton and Phelps¹¹ except for the different

"averaging" of $f_i(\nu)$. We also note from Eq. (14) that in order to obtain as large a signal as possible one should make $\Delta\nu$ as large as possible, e.g., use broad band filters rather than the narrow band filters used for line radiation. The filter transmission characteristics $f_i(\nu)$ and the detector responsivity $D(\nu)$ used in the calculations of C_{ff} were taken from manufacturer's specifications. The values of $k_{ff}(\nu)/k_{ff}(\nu_i)$ were calculated using the same theory as Rutscher and Pfau.⁶ The window transmission functions $f_r(\nu_i)$ and $f_w(\nu_i)$ are calculated from the indices of refraction. The correction for ionization and attachment was negligible for measurements in pure Ar.

It is important to keep in mind that throughout this paper we have not followed the usual convention of expressing the free-free emission in terms of a spectral intensity, i.e., cross section or excitation coefficient per unit spectral bandwidth, but rather have defined cross sections and rate coefficients per fractional bandwidth. This unconventional formulation has the advantages of yielding numbers which are independent of units used to measure bandwidth and of yielding cross sections and excitation coefficients which are readily compared with cross sections and excitation coefficients for the production of excited states which emit lines or molecular bands. In our experiments the fractional bandwidth of the detection system is typically 0.1.

III. EXPERIMENTAL APPARATUS AND PROCEDURE

The drift tube shown in the schematic of Fig. 1 is the same as the one used in references 4, 5 and 11. The electrode spacing was 38.4 mm and the cathode diameter was 60 mm. The accelerating voltage ranged from 100 to 1200 V and the total current in the on-period was 0.02 to 0.09 μA . Measurements are reported with 1 to 5% O_2 in Ar at the total gas densities of 10^{24} to $2 \times 10^{25} \text{ m}^{-3}$. After O_2 of 99.99% specified purity was admitted to the drift tube from a liquid- N_2 cooled, storage reservoir, Ar of nominal 99.999% purity was fed into the tube directly from a high pressure cylinder. The gases were allowed to mix for at least one half hour.

For measurements at $1.27 \mu\text{m}$ the period of the zero-based square wave voltage applied to the anode was varied from 10 to 25 sec depending on the decay constant of the $a^1\Delta_g$ state. This data recording period was followed by a dead time of 15 sec for the computer processing to be described later. A liquid- N_2 cooled intrinsic germanium detector had a responsivity and NEP (noise equivalent power) of $7 \times 10^9 \text{ V/W}$ and $1 \times 10^{-15} \text{ WHz}^{-1/2}$, respectively, at $1.3 \mu\text{m}$. The signal from the dc output of the detector for step function IR input signal consists of rapidly and slowly rising components, the time constants of which were about 10 msec and 3 sec, respectively. As described in detail in reference 4, this problem was overcome by using an amplifier containing differentiation and addition circuits which compensate for the 3 sec response and partially compensate for the 10 msec response. The compensation circuits were adjusted for a square wave output signal using the chopped signal from the black-body as an input signal.

A minicomputer was used as a data acquisition and analyzing system. The signal for the compensated amplifier was sampled every 40 to 100 msec

depending upon the period of the anode voltage. A set of data was stored in the computer and then analyzed to reject spikes due to cosmic rays.^{4,5} Ten to twenty sets of data were additively accumulated in the computer memory and then analyzed by a least-squares fitting procedure.

The measurement of the sensitivity of the detection system for infrared radiation emitted from the center of the collision chamber was made using a black-body source mounted on the opposite side of the drift tube from the detector. An aperture of 1.50 mm diameter was placed in front of the source 0.47 m from the detector so as to reduce the black-body signal. When the temperature of the source was 490 K the intensity at the detector was comparable to that observed for the $O_2(a^1\Delta_g)$ emission and was large compared to the thermal background signal. A chopper in front of the source modulated the black-body emission with a period of 20 sec, which was also comparable to that used for recording the $a^1\Delta_g$ emission. The spatial variation of the detection efficiency was measured using a small diffuse light source which was scanned over the drift region. The results of this type of measurement are summarized in the Appendix of reference 5.

The detection system and reference light source for the measurements of free-free emission at 500 and 700 nm was the same as that described by Lawton and Phelps.¹¹ An interference filter with 68% transmission and a band pass of 65 nm FWHM was used for the measurements reported for 500 nm. Measurements near 700 nm were made using a red-pass filter with 50% transmission at 670 nm and a uv sensitive, multialkali photomultiplier with a "cutoff" at about 800 nm. The principal difficulty encountered in these measurements was that of the calibration of the neutral density filters used to reduce the signal from the standard lamp to values in the linear range of the photon counting system. We estimate an uncertainty of $\pm 20\%$ for the resultant measured excitation coefficients.

IV. $O_2(a^1\Delta)$ EXCITATION COEFFICIENTS

In this Section we summarize the results of measurements of the coefficients for electron excitation of the $O_2(a^1\Delta)$ metastables in O_2 - N_2 -Ar mixtures and in O_2 - N_2 mixtures. As in our earlier measurements with O_2 -Ar mixtures, the Ar was used to reduce the loss of $O_2(a^1\Delta)$ molecules by diffusion to electrodes. Fortunately, the rate coefficient for the quenching of the $O_2(a^1\Delta)$ metastables by N_2 is low enough, i.e., about $8 \times 10^{-25} \text{ m}^3/\text{sec}$, so that it was possible to also make measurements using only the N_2 to limit the diffusion loss of the $O_2(a^1\Delta)$ metastables. Note that emission from the 1st positive band of N_2 near $1.3 \mu\text{m}$ is readily separated from the $O_2(a^1\Delta)$ emission because of the large difference in the decay time constants, i.e., the $N_2(B^3\Pi_g)$ lifetime¹⁵ is much shorter than that of the $O_2(a^1\Delta)$ metastables.

The results of our measurements of $O_2(a^1\Delta)$ excitation rate coefficients per oxygen molecule are shown by the points in Fig. 2 as a function of the mean electron energy $\langle \epsilon \rangle$ for various mixtures of O_2 , N_2 and Ar. This format was chosen to display the data since the excitation rate coefficients as a function of mean electron energy are expected to vary slowly with the gas mixtures. The measured α/N vs E/N values are converted into rate coefficients k vs $\langle \epsilon \rangle$ using theoretically calculated values of w and $\langle \epsilon \rangle$ vs E/N . The total gas densities used varied from 10^{25} m^{-3} at the lower E/N to $2 \times 10^{24} \text{ m}^{-3}$ at the higher E/N and higher N_2 concentrations.

The smooth curves of Fig. 2 show the calculated excitation coefficients for these mixtures. The calculations of the electron energy distributions, excitation coefficients drift velocities and mean energies were carried out using a modification of the electron- O_2 collision cross section set of

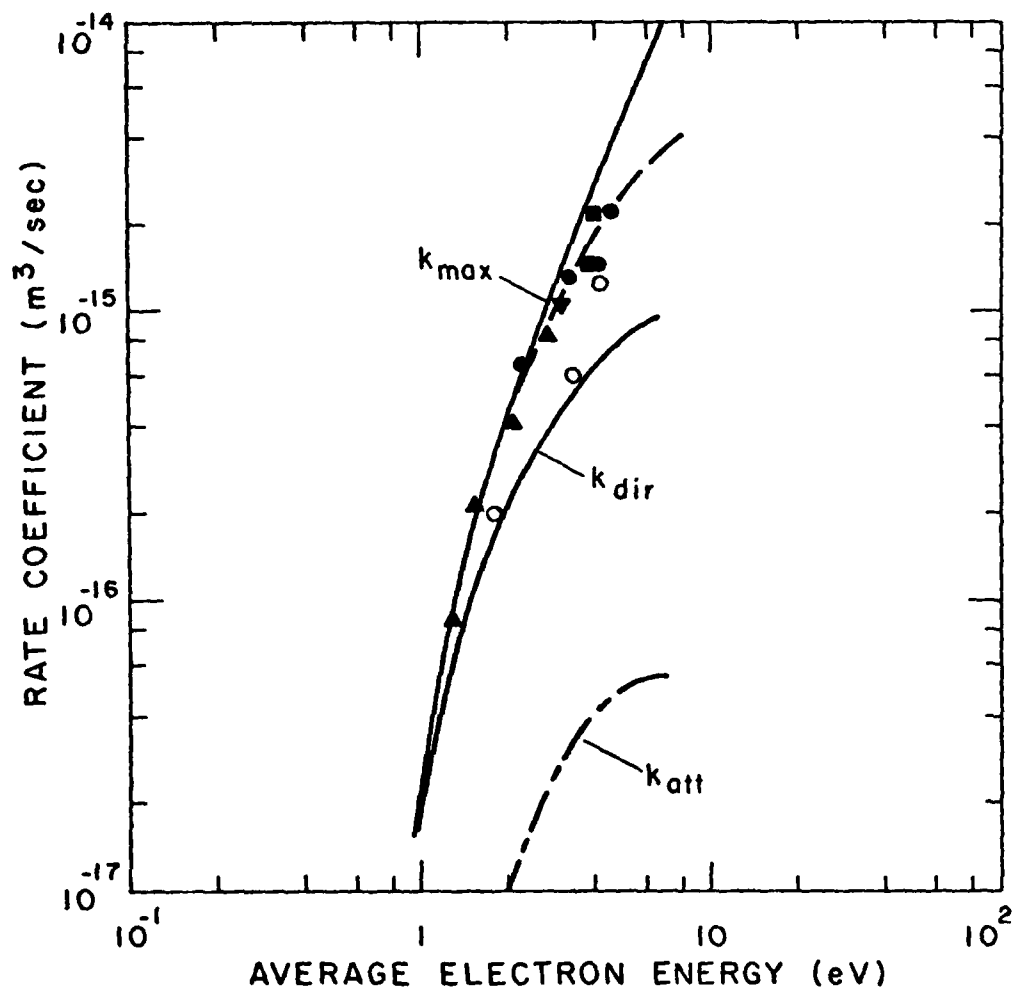


Figure 2. Rate coefficients per $O_2(a^1)$ metastables vs average electron energy in O_2-N_2-Ar mixtures. The symbols and the corresponding percentages of O_2 , N_2 and Ar are:
 ■, 1-1-98; ●, 1-2-97; ▼, 1-5-94; ▲, 2-10-88; ○, 5-5-90.

Lawton and Phelps¹¹ in which the relative vibrational excitation peaks were brought into better agreement with theory and their magnitudes adjusted to fit recent electron drift velocity data¹⁶ for O_2 and air at $\langle \epsilon \rangle < 0.3$ eV. The electronic excitation cross sections of importance here were unmodified. We used the electron- N_2 cross section set of Pitchford and Phelps;¹⁷ and the electron-Ar cross section set discussed by Tachibana and Phelps.⁵ The lower solid curve shows the predicted excitation coefficient under the assumption of only direct excitation of the $O_2(a^1\Delta)$ state, while the upper solid curve is calculated assuming that all of the electronically excited O_2 molecules cascade to the $a^1\Delta$ state. The dashed curve is calculated assuming that none of the $O(^1D)$ atoms formed by dissociative excitation of the $O_2(B^3\Sigma_u^-)$ state transfer their energy to the $O_2(b^1\Sigma)$ state and are subsequently collisionally deexcited to the $a^1\Delta$ state.

Collisional cascading efficiencies have been calculated using the rate coefficients given in Table 1 and are listed in Table 2 for various mixtures. In these calculations of the efficiency of excitation transfer from the $O(^1D)$ atoms it is assumed that all collisions with O_2 molecules lead to excitation of $O_2(b^1\Sigma)$ molecules. It is also assumed that the excitation of O_2 states represented by the 4.5 and 6.0 eV energy thresholds cascades to the $O_2(b^1\Sigma)$ state with 100% efficiency. At a mean electron energy of 2 eV excitation via the 4.5 and 6.0 eV states accounts for about 45% of the k_{\max} values shown in Fig. 2. The fractional efficiencies $F_1(^1\Sigma)$, $F_2(^1\Sigma)$ and $F_3(^1\Sigma)$ correspond to the quenching of $O_2(b^1\Sigma)$ molecules to the $O_2(X^3\Sigma)$ ground state by Ar and N_2 , by N_2 , and by Ar, respectively. Since the data obtained with 5% O_2 -5% N_2 -90% Ar appear to be inconsistent with the other

Table I
RATE COEFFICIENTS FOR COLLISIONAL DEEXCITATION
OF EXCITED OXYGEN*

Excited State Quencher	O ₂ (a ¹ Δ)	O ₂ (b ² Σ)	O(¹ D)
O ₂	1.5(-24) ^a	3.9(-23) ^b	4.1(-17) ^c
N ₂	2.2(-21) ^d	2.2(-12) ^d	3.0(-17) ^c
Ar	9(-27) ^a	1.5(-23) ^d	3(-18) ^e

* Here 1.5(-24) means 1.5×10^{-24} m³/sec

a) See Table I in reference 5

b) reference 11

c) reference 19

d) reference 20

e) reference 21

Table II
CALCULATED FRACTIONAL EXCITATION TRANSFER EFFICIENCIES*[‡]

% O ₂	% N ₂	% Ar	F(¹ D)	F ₁ (¹ Σ)	F ₂ (¹ Σ)	F ₃ (¹ Σ)
1	1	98	1.12(-1)	1.05(-1)	4.1(-1)	6.0(-1)
1	2	97	1.05(-1)	6.2(-3)	2.5(-1)	7.5(-1)
1	5	94	8.7(-2)	3.1(-3)	1.16(-1)	8.9(-1)
2	10	88	1.27(-1)	3.3(-3)	6.0(-2)	9.4(-1)
5	5	90	3.3(-1)	1.55(-2)	1.23(-1)	8.9(-1)
20	80	0	2.6(-1)	4.4(-3)	4.4(-3)	1
100	0	0	1	1	1	1

* 1.12(-1) means 1.12×10^{-1}

[‡] See text for definitions of symbols

data we will not consider them further. The remainder of the data is consistent with the assumption that all of the excitation of states up to and including the 6 eV state collisionally cascades to the $O_2(a^1\Delta)$ state.

The excitation rate coefficient data shown by the solid points of Fig. 2 for average electron energies above about 3 eV are consistent with inefficient excitation transfer from the $O(^1D)$ state to the $O_2(b^1\Sigma)$ state. Such low efficiencies are predicted in Table II, especially for the low fractional concentrations of O_2 which must be used at the higher $\langle \epsilon \rangle$ in order to avoid loss of electrons and, therefore signal, due to dissociative attachment of electrons to O_2 . The chain curve of Fig. 2 shows the dependence of the attachment rate coefficient k_{att} per O_2 molecule on the mean electron energy for these mixtures. A few measurements of $O_2(a^1\Delta)$ excitation coefficients were made in O_2-N_2 mixtures. The best results were obtained with 20% O_2 and 80% N_2 , a total gas density of $1.6 \times 10^{24} \text{ m}^{-3}$, and E/N between 8×10^{-21} and $8 \times 10^{-20} \text{ Vm}^2$. These results are compared with calculations of the $O_2(a^1\Delta)$ excitation coefficients in Fig. 3. Note that the coefficients shown are α/N values and thus are normalized to the total gas density N . The upper solid curve and the lower chain curve show the excitation coefficients predicted assuming 100% cascading and no cascading of higher excited states of O_2 to the $a^1\Delta$ state. The short dashed curve shows the calculated excitation coefficient assuming that none of the $O(^1D)$ atoms are able to form $O_2(b^1\Sigma)$ and, subsequently, $O_2(a^1\Delta)$ molecules. From the calculated excitation transfer efficiency $F(^1D)$ listed in Table II, we expect the experimental results to fall between the solid curve and the short dashed curve. The agreement

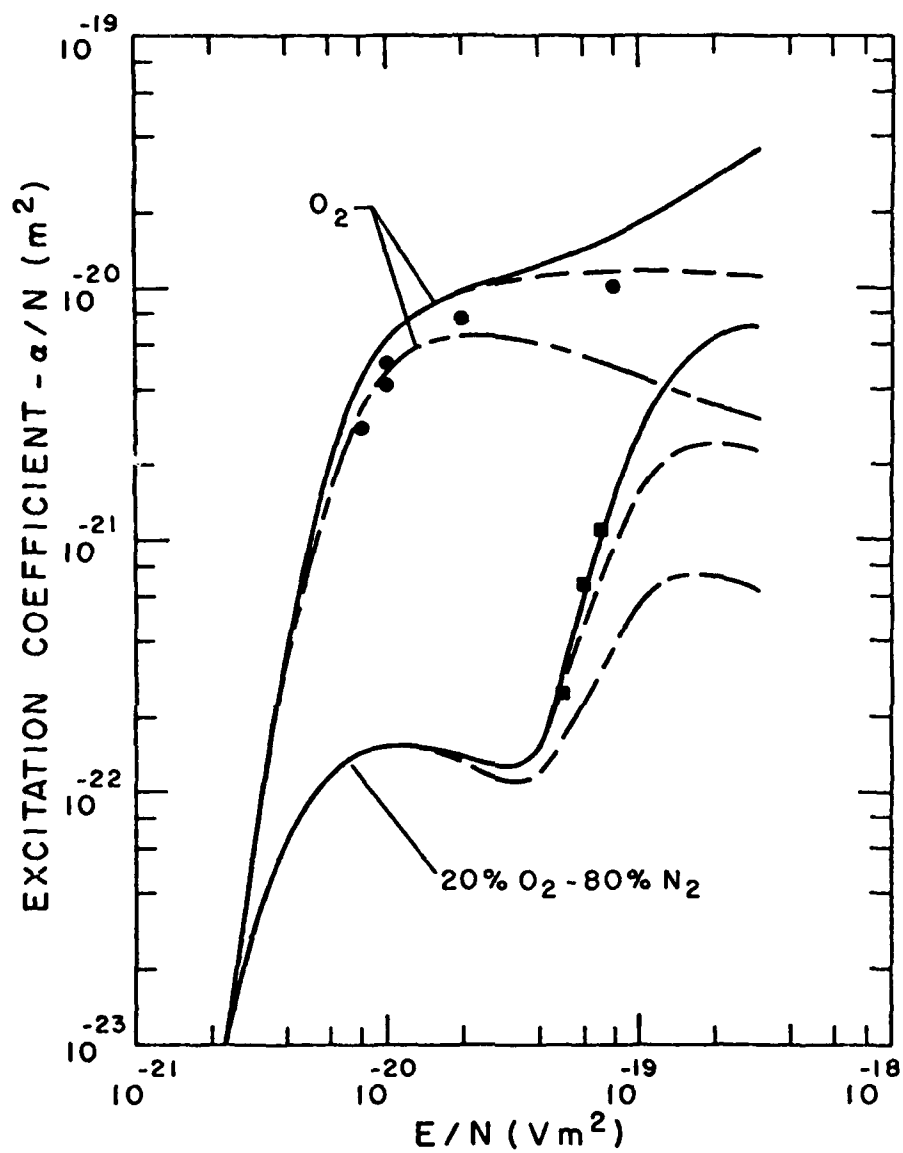


Figure 3. Excitation coefficients for production of $\text{O}_2(a^1\Delta)$ metastables in pure O_2 and in 20% O_2 - 80% N_2 .

between the measurements and the calculations is satisfactory when one considers the relatively poor signal to noise caused by the rapid loss of $O_2(a^1\Delta)$ molecules due to diffusion in the absence of the Ar buffer gas.

In one set of observations we measured the 1.27 μm emission from pure O_2 . In this case the O_2 density and E/N were varied from $N = 6.4 \times 10^{23} m^{-3}$ and $E/N = 8 \times 10^{-21} Vm^2$ to $N = 1 \times 10^{24} m^{-3}$ and $E/N = 7 \times 10^{-20} Vm^2$.

Since the time constants of the excited state decay were too short to measure at the low signal to noise ratios of these measurements, they were calculated from the other measurements of diffusion and collisional deexcitation coefficients.⁵ The values used were $3.9 sec^{-1}$ and $20 sec^{-1}$ at oxygen densities of 6.4×10^{23} and $1 \times 10^{24} m^{-3}$, respectively. The resultant experimental excitation coefficients for the $O_2(a^1\Delta)$ state by electrons in pure O_2 are compared with theoretical values in Fig. 3. As discussed above, the cross sections used in these calculations were modified from those of Lawton and Phelps.¹¹ We consider the agreement between experiment and theory to be satisfactory in view of the lack of measurements of the decay constant γ .

In our interpretation of the measurements of $O_2(a^1\Delta)$ excitation shown in Figs. 2 and 3, we have not considered the possible contributions from electronically excited N_2 . One such contribution to our observations could be the transfer of excitation from the electronically excited states of N_2 , e.g., the $A^3\Sigma$ state, to the $a^1\Delta$ state or to states of O_2 which cascade to the $a^1\Delta$ state. This process could have contributed about 30% of the signal observed at $E/N = 7 \times 10^{-20} Vm^2$ for the mixture of 20% O_2 and 80% N_2 as shown in Fig. 3. Zipf²² has recently observed efficient ($60 \pm 30\%$) formation of N_2O in the collisions of $N_2(A^3\Sigma)$ with O_2 , so that alternate deexcitation paths are available. Deexcitation of the $N_2(A^3\Sigma)$ molecules by N_2 is slow²³ and can be neglected in our experiment.

V. FREE-FREE EMISSION COEFFICIENTS

In this section we summarize the results of measurements of the free-free emission coefficients for electrons in Ar. Figure 4 shows an example of the infrared emission signals which led to the conclusion that the drift tube technique could be used to measure free-free emission coefficients. This waveform was obtained during measurements of $O_2(a^1\Delta)$ production in a mixture of 0.05% O_2 in Ar at a total gas density of 10^{25} m^{-3} and an E/N of $3 \times 10^{-21} \text{ Vm}^2$. The exponentially rising and falling portions of this waveform are interpreted as emission from $O_2(a^1\Delta)$ molecules at $1.27 \text{ }\mu\text{m}$ and yield excitation coefficients consistent with those reported in references 4 and 5. When the exponentially varying portions are subtracted from the observed waveform one is left with a rectangular waveform which we interpret as free-free emission emitted in collisions between electrons and argon atoms. This interpretation is supported by the results of measurements in pure Ar. In this case only the rectangular component of the waveform was observed.

Averaged values of free-free emission coefficients for pure Ar at wavelengths near $1.3 \text{ }\mu\text{m}$ are calculated from the observed magnitude of the infrared signal using Eq. (16) and are shown as a function of E/N by the squares in Fig. 5. Similarly, the triangles and the circles of Fig. 5 show the averages of results of measurements near 700 and 900 nm, respectively. A better indication of the spread in the experimental data is obtained from the linear plots of free-free emission coefficient versus wavelength for E/N values of $3 \times 10^{-21} \text{ Vm}^2$ (squares) and $2 \times 10^{-21} \text{ Vm}^2$ (triangles) in Fig. 6.

In order to compare the various theoretical predictions of free-free emission for electrons in argon, we have shown in Fig. 7 the theoretical

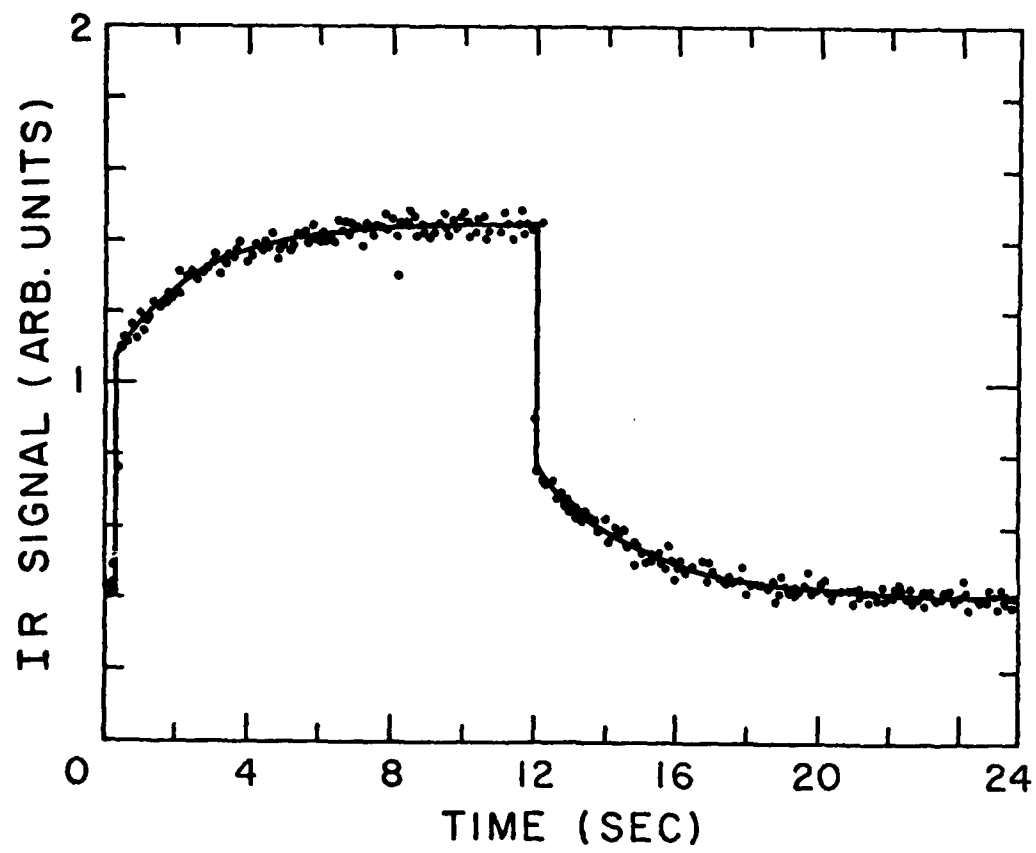


Figure 4. Infrared emission transient near $1.3 \mu\text{m}$ from $0.05\% \text{ O}_2$ in Ar.

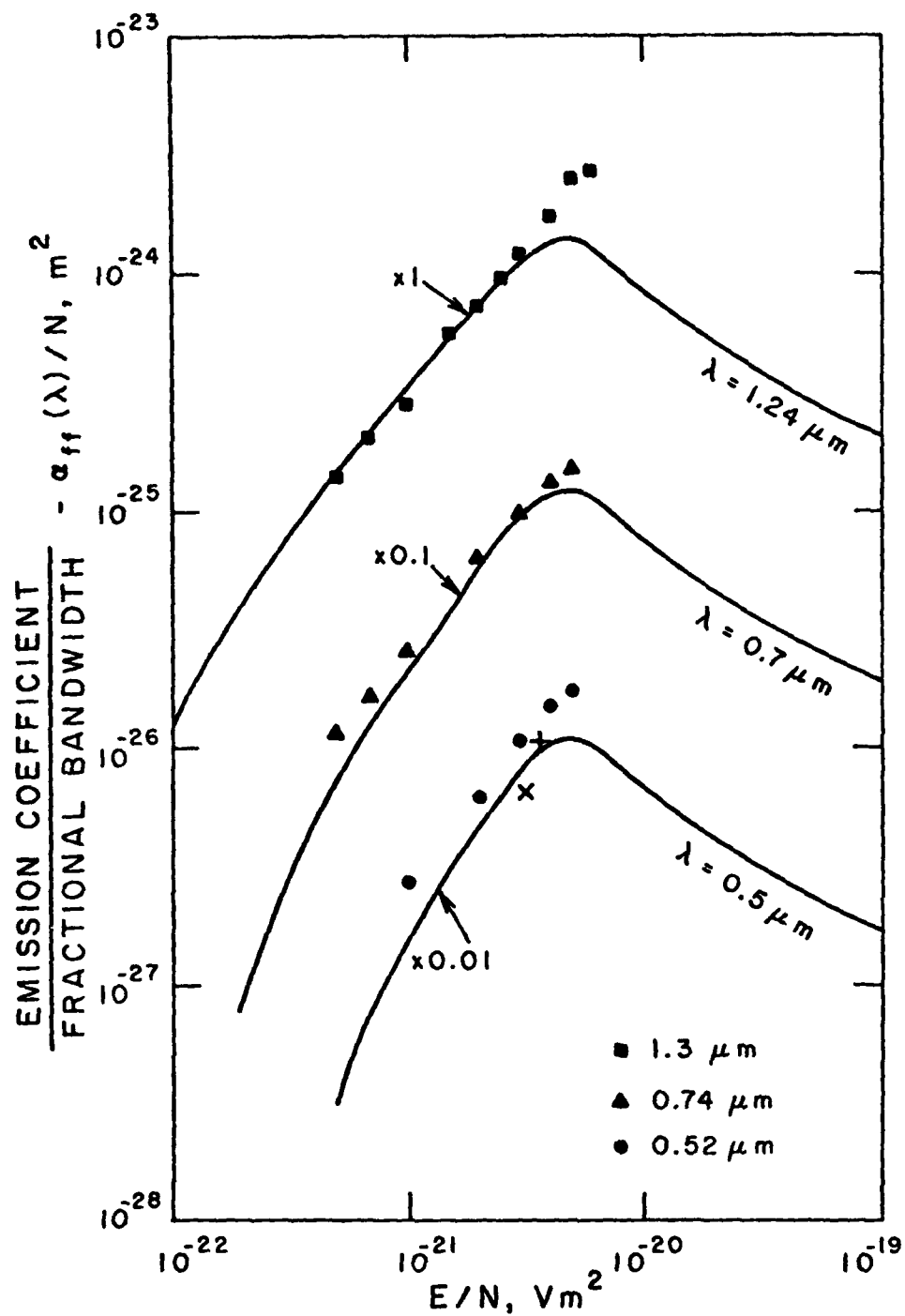


Figure 5. Free-free emission coefficient per fractional bandwidth for electrons in argon vs E/N . The + and x are from references 30 and 31, respectively.

cross sections for this process as a function of electron energy. The cross section $Q_B(\epsilon, h\nu)$ is that for the production by electron of energy ϵ of photons of a particular energy $h\nu$ (1.78 eV) per unit fractional band width. The Rutscher and Pfau⁶ expression for this cross section is

$$Q_{ff}(\epsilon, h\nu) = \frac{4}{3\pi} \frac{\alpha^3}{Ry} \frac{(\epsilon - h\nu/2)(\epsilon - h\nu)^{1/2}}{1/2} Q_m(\epsilon) \quad , \quad (19)$$

where α is the fine structure constant and Ry is the Rydberg (13.6 eV). Our calculations of $Q_{ff}(\epsilon, h\nu)$ using Eq. (19) are shown for a photon energy of 1.77 eV by the points in Fig. 7. As in reference 5, the momentum transfer cross sections used in these calculations were those of Milloy, et al.²⁴ below 4 eV; those of Fletcher and Burch²⁵ above 8 eV; and a smooth interpolation at intermediate electron energies. The solid curve is interpolated from tabular cross sections obtained by Geltman,²⁶ while the dashed curve is calculated from the absorption coefficients obtained by Askin.²⁷ Other calculations of free-free transition for argon²⁸ do not present results suitable for this comparison. Since the differences among these theoretical cross sections are well within our experimental scatter, we have used Eq. (19) in the remainder of this investigation.

The solid curves of Figs. 5 and 6 are the result of calculations of free-free emission coefficients which we have made using Eq. (19) for the free-free emission cross section and the electron energy distributions which we have calculated. Thus, Eq. (7) can be written as

$$k_{ff} = w_e \alpha_{ff} / N = \left(\frac{m}{2} \right)^{1/2} \int_h^\infty \epsilon Q_{ff}(\epsilon) f(\epsilon) d\epsilon \quad . \quad (20)$$

Our electron energy distributions were calculated using the electron-Ar collision cross section data discussed above and in reference 5.

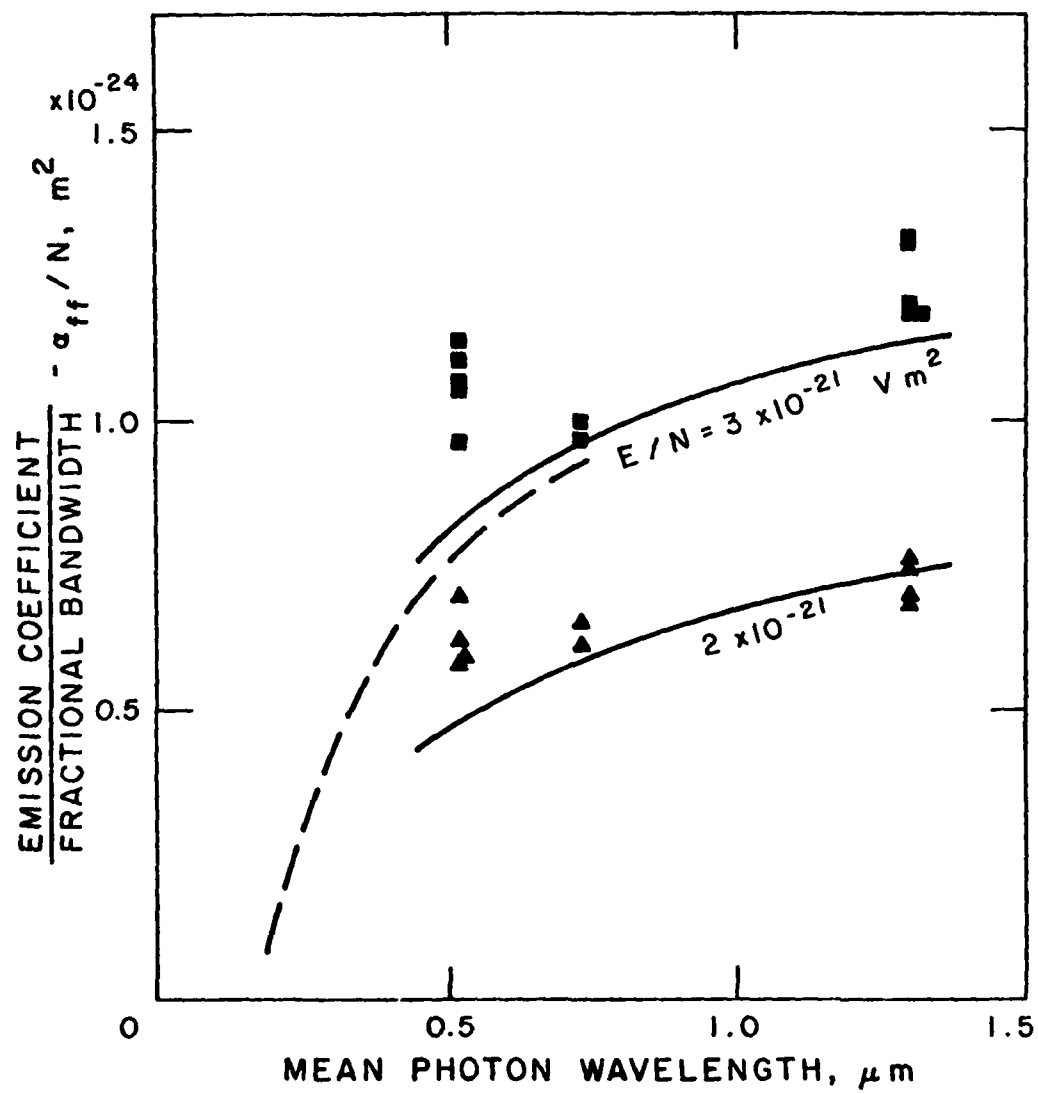


Figure 6. Wavelength dependence of free-free emission coefficient per fractional bandwidth for electrons in Ar.

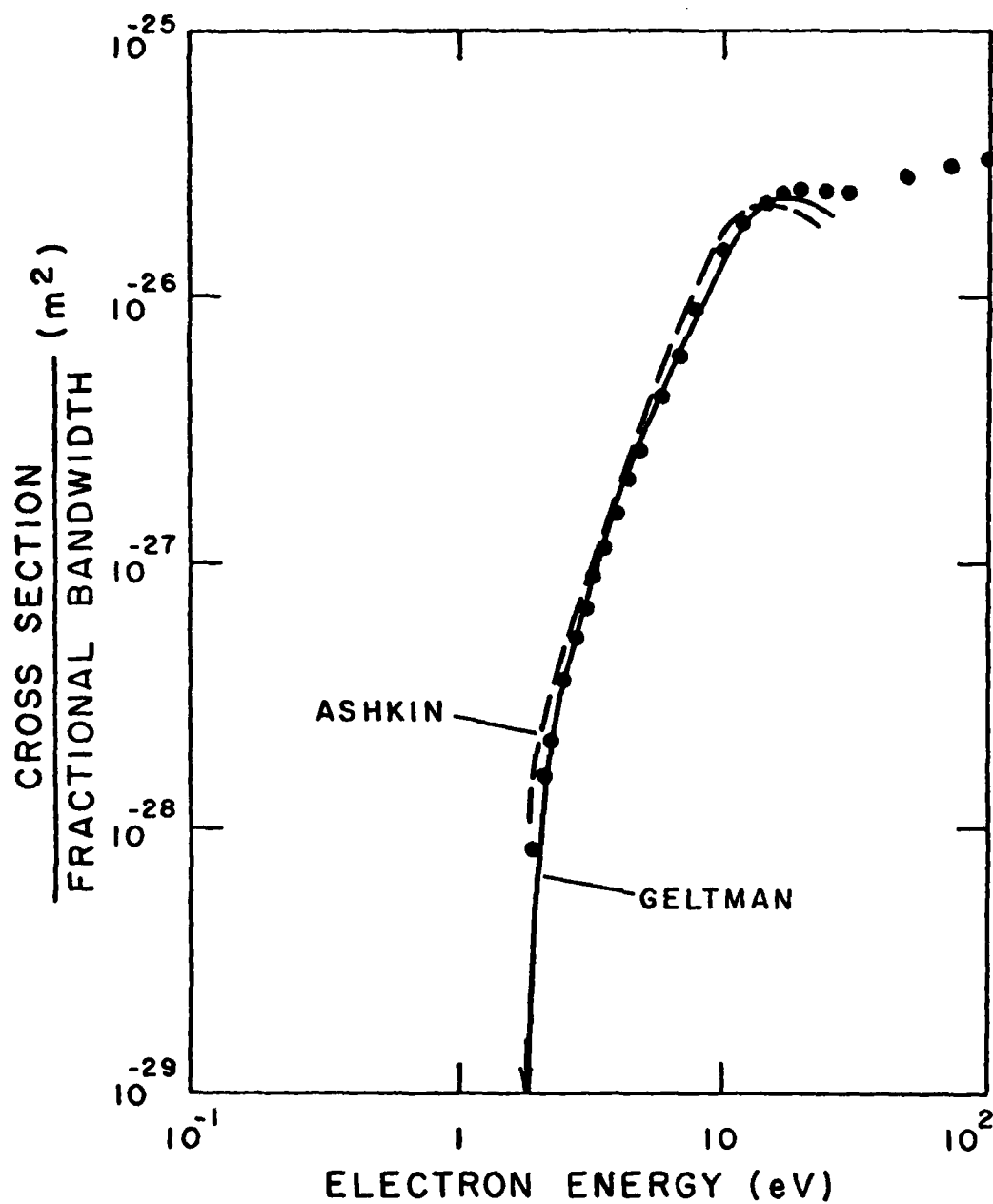


Figure 7. Theoretical cross section per fractional bandwidth for the emission of 1.78 eV photons vs electron energy.

The dashed curve of Fig. 6 was obtained by interpolation of graphs of calculations by Pfau, Rutscher and Winker.⁶ The somewhat lower emission coefficients obtained by these authors are presumably the result of the use of somewhat larger electron-Ar collision cross sections with a resultant lower mean electron energy at a fixed E/N.

The agreement between experiment and theory is generally better at longer wavelengths and lower E/N. The relatively large experimental coefficients at E/N values above $4 \times 10^{-21} \text{ Vm}^2$ at 700 nm and 1.3 μm are probably the results of the emission of line radiation by highly excited Ar atoms. This excess emission was even more pronounced in data obtained at 1.3 μm in O_2 -Ar mixtures, when the E/N was raised to values very close to those causing electrical breakdown.

The generally good agreement between experiment and theory, i.e., discrepancies of less than 25%, shown in Fig. 6 is in contrast to the factor of three to four discrepancy found using the shock tube technique.²⁹ Absolute measurements of free-free emission signals from electrical discharges in Ar are reported for wavelengths from 300 to 500 nm by Vasileva, Zhidanova and Mnatsakanyan³⁰ and for 480 nm by Golubovskii, Kagan and Komarova³¹ were about $(75 \pm 20\%)$ and $(100 \pm 20\%)$, respectively of their theoretical values. Representative data obtained by these authors is shown in Fig. 5. This agreement is remarkably good when one considers the problems of the determination of the electron density and of the effects of electron-electron collisions and of gas heating on the analysis of their data, and when one notes the approximate calculations of the electron energy distributions, etc., which they used. A significant advantage of these discharge experiments is the emission of much larger ($\sim 10^5$) signals than for our experiments. The results of Vasileva, et al.³⁰ and of Rutscher and Pfau⁶ provide the best checks of the theoretical predictions of the wavelength dependence of the free-free emission.

VI. SUMMARY AND RECOMMENDATION

The results presented in Section IV of this report for O_2 - N_2 -Ar and O_2 - N_2 mixtures and pure O_2 are consistent with our previous results for O_2 -Ar mixtures in that the use of the recommended electronic excitation cross section set for O_2 of Lawton and Phelps¹¹ yields excitation coefficients for the $a^1\Delta_g$ state of O_2 in reasonable agreement with experiment. Furthermore, the results are consistent with the efficient collisional quenching of higher excited states of O_2 molecules to the $O_2(a^1\Delta)$ state via the $O_2(b^1\Sigma)$ state as proposed by Lawton and Phelps. At the highest electron mean energies used the results are consistent with the interception of the cascading via the $O(^1D)$ state in collisions with Ar atoms and N_2 molecules.

The results presented in this report provide relatively little information regarding the vibrational excitation of the O_2 molecule. This conclusion is the result of the fact that the measurements were made at mean electron energies where the dominant excitation process for O_2 were production of molecules in the electronically excited states. We therefore plan to continue with the measurements of the vibrational excitation of O_2 . As discussed in our proposal, we will make use of the resonant transfer of excitation of vibrational excitation from O_2 to the asymmetric stretch mode of CS_2 , with the subsequent emission of radiation near $6.5 \mu m$.³²

The results presented in Section V of this report show, for the first time, the usefulness of the electron drift tube technique for the measurement of free-free emission coefficients for electrons in gases. As shown by our results, this technique makes possible measurements of free-free emission coefficients under much more accurately known experimental conditions for a wide selection of mean electron energies (1.6 to 4.2 eV) than

was possible using the discharge technique and leads to much more reproducible results than does the shock tube technique. The free-free emission coefficients presented in this report for electrons in argon are in agreement with theoretical values to within the present experimental uncertainty. It is recommended that these measurements be extended to molecular gases of Air Force interest, e.g., N_2 , and that efforts be made to improve the measurement techniques so as to extend the range of mean electron energies downward.

APPENDIX: Evaluation of G_{ff}

In this appendix we write down specific forms of the geometrical factor G_{ff} defined by Eq. (10), i.e.,

$$G_{ff} = \frac{\int_0^L n_e \eta dz}{\int_0^L n_e dz} \quad (A1)$$

Since for these experiments

$$n_e = n_0 e^{-\alpha z}$$

we find

$$G_{ff} = \frac{a}{(1-e^{-a})L} \int_0^L e^{-\alpha z} \eta(z) dz \quad (A2)$$

where $a = (\alpha - \alpha_1)L$.

In general one can write

$$\eta(z) = \sum P_n \cos(n\pi z/L) + \sum Q_n \cos(n\pi z/L) \quad (A3)$$

and

$$G_{ff} = \frac{a}{(1-e^{-a})} \left[\sum \frac{a P_n (1-n\pi e^{-a})}{a^2 + (n\pi)^2} + \sum \frac{n\pi Q_n (1+e^{-a})}{a^2 + (n\pi)^2} \right] \quad (A4)$$

For the typical case of

$$\eta = A + B \sin \pi z/L + C(1-2z/L) \quad (A5)$$

the results of Lawton and Phelps⁷ reduce to

$$G_{ff} = A + \frac{B\pi a(e^a+1)}{(a^2+\pi^2)(e^a-1)} + C \left[\frac{(1-e^{-a})}{(1-e^{-a})} - \frac{2}{a} \right] \quad (A6)$$

REFERENCES

1. R. D. Hake, Jr. and A. V. Phelps, Phys. Rev. 158, 70 (1967).
2. A. Napartovich, V. G. Naumov and V. M. Shashov, Fiz. Plazmy 1, 821 (1975) [Sov. J. Plasma Phys. 1, 449 (1975)].
3. W. E. McDermott, N. R. Pchelkin, D. J. Benard, and R. R. Bousek, Appl. Phys. Lett. 32, 469 (1978); D. J. Benard, W. E. McDermott, N. R. Pchelkin, and R. R. Bousek, Appl. Phys. Lett. 34, 40 (1979); G. Fournier, J. Bonnet, and D. Pigache, 3rd Int'l. Symp. on Gas Flow and Chemical Lasers, Marseille, September 1980.
4. K. Tachibana and A. V. Phelps, Final Report AFWAL-TR-81-2038, Air Force Wright Aeronautical Laboratory, May 1981.
5. K. Tachibana and A. V. Phelps, J. Chem. Phys. 75, 3315 (1981).
6. G. A. Rutscher and S. Pfau, Physica 81c, 395 (1976).
7. R. Winkler, P. Michel, and J. Wilhelm, Beit. Plasmaphysik 18, 31 (1978); S. Alroy and W. H. Christiansen, Appl. Phys. Lett. 32, 607 (1978); V. V. Minin, V. E. Tretyakov, and B. P. Yatsenko, Int'l. Conf. on the Physics of Ionized Gases, Minsk, USSR, 1981, p. P1731.
8. J. C. Morris, R. U. Krey, and G. R. Bach, J. Quant. Spectrosc. Radiat. Transfer 6, 727 (1966); L. M. Biberman and G. E. Norman, Ysp. Fiz. Nauk. 91, 52 (1967) [Sov. Phys. Usp. 10, 52 (1967)]; J. C. Morris, R. U. Krey, and R. L. Garrison, Phys. Rev. 180, 167 (1969).
9. R. M. Badger, A. C. Wright, and R. F. Whitlock, J. Chem. Phys. 43, 4345 (1965).
10. C. W. Cho, E. J. Allen, and H. L. Welsch, Can. J. Phys. 41, 1991 (1963).
11. S. A. Lawton and A. V. Phelps, J. Chem. Phys. 69, 1055 (1978).
12. H. C. Wood, W.F.J. Evans, E. J. Llewellyn, and A. Valence Jones, Can. J. Phys. 48, 862 (1970).
13. S. Pfau and A. Rutscher, Ann. der Physik 22, 166 (1969); S. Pfau, A. Rutscher, and R. Winkler, Beit. Plasmaphys. 16, 317 (1976).
14. Yu. B. Golubovskii, Yu. M. Kagan, P. Michel, and L. L. Nesterowa, Beit. Plasmaphys. 9, 217 (1969); Yu. B. Golubovskii, V. A. Ivanov, and Yu. M. Kagan, Opt. Spectrosc. 35, 213 (1973) [Opt. Spectrosc. 35, 124 (1973)].
15. R. F. Heidner, III, D. G. Sutton, and S. N. Suchard, Chem. Phys. Lett. 37, 243 (1976).
16. I. D. Reid and R. W. Crompton, Aust. J. Phys. 33, 215 (1980); R. Hegerberg and I. D. Reid, *ibid* 33, 226 (1980).
17. L. C. Pitchford and A. V. Phelps, 34th Gaseous Electronics Conf., Boston, October 1981.

18. P. Borrell, P. M. Borrell, and M. D. Pedley, Chem. Phys. Lett. 51, 300 (1977);
19. J. A. Davidson, C. M. Sadowski, H. I. Schiff, G. E. Streit, C. J. Howard, D. A. Jennings, and L. A. Schmeltekopf, J. Chem. Phys. 64, 57 (1976).
20. J. A. Davidson and E. A. Ogryzlo, in Chemiluminescence and Bioluminescence, ed. by M. J. Cormier, D. M. Hercules, and J. Lee (Plenum, New York, 1973), p. 111.
21. K. F. Preston and R. J. Cvetanović, J. Chem. Phys. 45, 2888 (1966).
22. E. C. Zipf, Nature 287, 523 (1980).
23. D. Levron and A. V. Phelps, J. Chem. Phys. 69, 2260 (1978).
24. H. B. Milloy, R. W. Crompton, J. A. Rees, and A. G. Robertson, Aust. J. Phys. 30, 61 (1977).
25. J. Fletcher and D. S. Burch, J. Phys. D 5, 2037 (1972).
26. S. Geltman, J. Quant. Spectrosc. Radiat. Transfer, 13, 601 (1973), and private communication.
27. M. Ashkin, Phys. Rev. 141, 41 (1966).
28. J. R. Stallcop, Astron. and Astrophys. 30, 293 (1974); M. S. Pindzola and H. P. Kelly, Phys. Rev. A 14, 204 (1976).
29. R. L. Taylor and G. Caledonia, J. Quant. Spectrosc. Radiat. Transfer 9, 657 (1969); R.T.V. Kung and C. H. Chang, *ibid* 16, 579 (1976).
30. I. A. Vasileva, Yu. Z. Zhandova and A. Kh. Mnatsakanyan, Opt. Spektrosk. 29, 644 (1970) [Opt. Spectrosc. 29, 345 (1970)].
31. Yu. B. Golubovski, Yu. M. Kagan, and L. L. Komarova, Opt. Spektrosk. 34, 226 (1973) [Opt. Spectrosc. 34, 127 (1973)].
32. J. K. Handcock, D. F. Starr, and W. H. Green, J. Chem. Phys. 61, 3017 (1974); D. C. Richman and R. C. Millikan, *ibid* 61, 4263 (1974).

**DATE
FILMED**

7-8